Journal of Rock Mechanics and Geotechnical Engineering xxx (xxxx) xxx

Contents lists available at ScienceDirect

Journal of Rock Mechanics and Geotechnical Engineering

journal homepage: www.jrmge.cn

Full Length Article

Effect of CO_2 exposure on the mechanical strength of geopolymer-stabilized sandy soils

Hamid Reza Razeghi [a,*], Armin Geranghadr [a], Fatemeh Safaee [a], Pooria Ghadir [a,b], Akbar A. Javadi [b]

[a] School of Civil Engineering, Iran University of Science and Technology, Tehran, 1684613114, Iran
[b] Department of Engineering, University of Exeter, Exeter, EX4 4QF, UK

ARTICLE INFO

Article history:
Received 4 December 2022
Received in revised form
12 April 2023
Accepted 12 April 2023
Available online xxx

Keywords:
Soil stabilization
CO_2 effect
Geopolymer

ABSTRACT

In recent years, there has been growing interest in developing methods for mitigating greenhouse effect, as greenhouse gas emissions continue to contribute to global temperature rise. On the other hand, investigating geopolymers as environmentally friendly binders to mitigate the greenhouse effect using soil stabilization has been widely conducted. However, the effect of CO_2 exposure on the mechanical properties of geopolymer-stabilized soils is rarely reported. In this context, the effect of CO_2 exposure on the mechanical and microstructural features of sandy soil stabilized with volcanic ash-based geopolymer was investigated. Several factors were concerned, for example the binder content, relative density, CO_2 pressure, curing condition, curing time, and carbonate content. The results showed that the compressive strength of the stabilized sandy soil specimens with 20% volcanic ash increased from 3 MPa to 11 MPa. It was also observed that 100 kPa CO_2 pressure was the optimal pressure for strength development among the other pressures. The mechanical strength showed a direct relationship with binder content and carbonate content. Additionally, in the ambient curing (AC) condition, the mechanical strength and carbonate content increased with the curing time. However, the required water for carbonation evaporated after 7 d of oven curing (OC) condition and as a result, the 14-d cured samples showed lower mechanical strength and carbonate content in comparison with 7-d cured samples. Moreover, the rate of strength development was higher in OC cured samples than AC cured samples until 7 d due to higher geopolymerization and carbonation rate.

1. Introduction

In recent years, world energy consumption (coal, oil, and natural gas, etc.) has been increasing and industrialization has led to high amounts of CO_2 emissions. Moreover, the construction industry has caused excessive CO_2 emissions because of using non-environmentally friendly materials like Portland cement. As a result, the researchers' attention has been drawn to the methods of reducing CO_2 and mitigating the greenhouse effect. One of the main methods of mitigating CO_2 effectis carbonation which involves the chemical reaction of carbon dioxide to give carbonates, bi-carbonates, and carbonic acid (Pavithra et al., 2016; Ruan and Unluer, 2016; Wang et al., 2019; Mohammed et al., 2021). Natural carbonation, which can be referred to as weathering, involves the removal of atmospheric CO_2 through the reaction of CO_2 and natural alkali silicates to form carbonates (Lim et al., 2010; Santos et al., 2021).

Lu et al. (2011) conducted test on natural basalt samples to determine the amount of CO_2 trapped by natural carbonation reactions. Based on a semi-quantitative estimate, 94.15 kg of CO_2 per 1 m^3 of basalt was trapped. However, due to the very low concentration of atmospheric CO_2 (0.03%–0.06%), the carbonate kinetics naturalization was very slow and did not have much effect on reducing the concentration of CO_2 in the atmosphere (He et al., 2011; Lu et al., 2011).

Another research used accelerated carbonation as a method of CO_2 removal, in which high-purity CO_2 was artificially injected into alkaline materials to enhance the carbonation reaction to produce stable carbonates on a time scale of a few hours (Lim et al., 2010).

* Corresponding author.
E-mail address: razeghi@iust.ac.ir (H.R. Razeghi).
Peer review under responsibility of Institute of Rock and Soil Mechanics, Chinese Academy of Sciences.

https://doi.org/10.1016/j.jrmge.2023.04.017

Please cite this article as: Razeghi HR et al., Effect of CO_2 exposure on the mechanical strength of geopolymer-stabilized sandy soils, Journal of Rock Mechanics and Geotechnical Engineering, https://doi.org/10.1016/j.jrmge.2023.04.017

Accelerated carbonation is divided into two main types including mineral carbonation and alkaline solid waste carbonation (Lim et al., 2010). The process of mineral carbonation contains the removal of CO_2, including the reaction of basic minerals (which includes a high concentration of calcium or magnesium oxide) or natural minerals (olivine, wollastonite, and serpentine) with high-purity of CO_2. This turns into stable carbonate in the presence of high temperature and pressure (Huijgen et al., 2006). This method has the potential to remove high concentrations of CO_2. However, it is very costly due to the high amount of energy required to crush raw materials to compress the CO_2 feed into the raw slurry, as well as the energy required to reach high temperatures (Huijgen et al., 2006; Lu et al., 2011). Alkaline waste carbonation is a CO_2 removal method that involves a one-step reaction (also called direct carbonation) of high-purity CO_2 with solid alkaline waste to produce carbonates (Washbourne et al., 2012). Alkaline waste carbonation does not require the extraction of active cations because cation-containing oxides, hydroxides, and silicates are the main reactive phases involved in this process (Washbourne et al., 2012; Papa et al., 2019). Blast furnace slag, cement kiln dust (CKD), construction and demolition waste, steel slag (SS), and ash of incinerated municipal solid waste are some of the alkaline wastes that have been successfully used in this carbonation process (Washbourne et al., 2012).

In another study, the effects of temperature, CO_2 pressure and carbonation time on the compressive strength, CO_2 sequestration, mineralogy and microstructure of steel slag block were investigated. It was concluded that higher temperatures than 70 ° C led to less formation of $CaCO_3$ and lower compressive strength because of water evaporation and reduced CO_2 solubility (Zhong et al., 2021).

In recent years, geopolymers have been widely used instead of cement, due to their environmentally friendly features and low production cost (Mola-Abasi and Shooshpasha, 2016; Ghadir and Ranjbar, 2018; Ghadir et al., 2021). Geopolymers are integrated from the chemical reaction between an amorphous predecessor, which possesses sufficient alumina (Al_2O_3) and silicate (SiO_2), with a sodium- or potassium-based activator (Xu and Van Deventer, 2000; Miraki et al., 2022; Razeghi et al., 2022). In summary, geopolymer or inorganic polymer formation employs reusable industrial waste materials (e.g. ground granulated blast-furnace slag) or mineral materials (e.g. volcanic ash) as a supply of silicon (Si) and aluminum (Al). The Si and Al break up in an alkaline activating solution, and after that, the molecules of silicon, aluminum, and oxygen make a chain of silicates and alumina tetrahedra that sporadically unite together by sharing oxygen atoms, which are transformed into three-dimensional polymeric Si-O-Al-O at nanoscale (Shariatmadari et al., 2021a; Samadi et al., 2023). At the beginning, some geopolymer precursors such as volcanic ash were used as an additive to cement. In recent years, the use of geopolymer instead of Portland cement has been noticed in soil stabilization because in addition to CO_2 capturing potential and mitigating greenhouse effect, it can stabilize problematic soil to an acceptable level depending on the duration and location conditions of the project. A lot of studies have been conducted on the stabilization of problematic soils with geopolymers. It shows that according to the limitations and conditions of the project, it is possible to choose the appropriate precursor and activator and stabilize the problematic soil (Miraki et al., 2022; Razeghi et al., 2022). In recent years, different precursors have been studied as geopolymer precursors for soil stabilization, including fly ash, blast furnace slag, metakaolin, and volcanic ash. For instance, a study was conducted on the feasibility of using metakaolin instead of Portland cement for soil stabilization and it was proved that the mechanical properties of metakaolin geopolymer stabilized soil can even surpass the mechanical properties of Portland cement stabilized soil. Also, it has been shown that the metakaolin stabilized soil has less brittleness than the unimproved sample, so it can be a suitable option for paving roads (Zhang et al., 2013).

Another research describes an innovative approach to stabilize soil surfaces against wind erosion using volcanic ash-based geopolymer. The authors experimentally investigated the effectiveness of the geopolymer in stabilizing wind-susceptible soil surfaces. The results showed that the geopolymer significantly improved the soil's resistance to wind erosion, reducing the soil's erosion rate by up to 99.7%. The geopolymer also improved the soil's water retention capacity and reduced its susceptibility to crusting. The study found that the geopolymer's effectiveness in stabilizing soil surfaces was dependent on factors such as the geopolymer's composition, application rate, and curing time. The authors concluded that volcanic ash-based geopolymer has the potential to be an effective and sustainable solution for soil stabilization against wind erosion, particularly in arid and semi-arid regions (Shariatmadari et al., 2021b).

Mohebbi et al. (2022) investigated the use of a volcanic ash-based geopolymer as a surface stabilizer by studying the rheological behavior of different geopolymer mix designs. A shear-thinning behavior was identified in all samples, and a linear correlation was found between the final apparent viscosity and the binder-to-activator ratio. The chemical features of mix design and infiltration depth were found to have a major influence on the final resistance of geopolymer-treated soils, regardless of the effect of binder content on soil structure.

Another promising characteristic of the geopolymer is CO_2 capturing potential in order to produce carbonate and bicarbonate compounds desirable for soil stabilization addition to mitigation of greenhouse effect (Fasihnikoutalab et al., 2016, 2017b). Ground granulated blast furnaces slag (GGBS), volcanic ash, and olivine, etc. have been widely suggested for direct carbonation (Fasihnikoutalab et al., 2016).

Fasihnikoutalab et al. (2016) conducted a laboratory-scale model for soil stabilization using carbon dioxide (CO_2) deposition. The authors investigated the effectiveness of CO_2 deposition in stabilizing soil samples under different conditions, such as different CO_2 flow rates, durations, and soil types. The results showed that CO_2 deposition significantly improved the soil's compressive strength and reduced its permeability. The study also found that the effectiveness of CO_2 deposition was dependent on factors such as soil type, CO_2 flow rate, and deposition duration. Fasihnikoutalab et al. (2017b) investigated the use of alkali-activated olivine as a soil stabilizer and the effect of carbonation on its strength and microstructure. The results showed that alkali-activated olivine significantly improved the soil's mechanical properties and reduced its permeability. The study also found that carbonation had a positive effect on the strength of alkali-activated olivine-stabilized soil, with the strength increasing over time due to the formation of carbonate minerals. The authors concluded that alkali-activated olivine can be a promising and sustainable solution for soil stabilization, and carbonation process can further enhance its effectiveness.

Although various researches were conducted on the effect of the carbonation process on Portland cement stabilized soils, the effect of CO_2 exposure on the mechanical strength of geopolymer stabilized soils has not yet been fully understood. The present study attempts to fill the gaps in the available literature and develops an in-depth understanding of the effect of CO_2 exposure on mechanical and microstructural features of a sandy soil stabilized with volcanic ash-based geopolymer. The carbonate content was assessed by calcimeter and the intensity of its crystalline phases was elaborated using the analysis of X-ray diffraction (XRD) patterns in both ambient curing (AC) and oven curing (OC) conditions. The chemical bond structures and the variation of the amorphous

Please cite this article as: Razeghi HR et al., Effect of CO_2 exposure on the mechanical strength of geopolymer-stabilized sandy soils, Journal of Rock Mechanics and Geotechnical Engineering, https://doi.org/10.1016/j.jrmge.2023.04.017

bonds were further analysed using FTIR spectroscopy. Also, scanning electron microscope (SEM), energy-dispersive spectroscopy (EDS), and mapping analysis were used to evaluate specimens' matrices.

2. Materials and methods

2.1. Soil characterization

The soil employed in this context was Firouzkouh sand (No. 161) sampled from the Firouzkouh mine, northeast of Tehran, Iran. Fig. 1 illustrates the grain size distribution of the sand based on the ASTM D422-63 (2002). Based on the Unified Soil Classification System (USCS), the soil is categorized as poorly graded sand (SP). Standard Proctor compaction tests were carried out on the soil to obtain the maximum dry density (γ_{max}) based on ASTM D698-21 (2021). The minimum and maximum densities were 1.397 g/cm^3 and 1.635 g/cm^3, respectively. Tables 1 and 2 show the physical characteristic and the results of the X-ray fluorescence (XRF) test for the sand, respectively.

2.2. Binders characterization

Volcanic ash is a characteristic pozzolanic material. In recent years, there has been an increasing interest in the utilization of volcanic ash (Tchakoute Kouamo et al., 2013b; Cai et al., 2016; Cheng-Yong et al., 2017). This natural material is found broadly through the world and has numerous normal highlights like being a rich source of aluminosilicate (Djobo et al., 2017; Ghadir et al., 2021). The volcanic ash utilized in this study was obtained from Taftan Mountain in Sistan and Baluchestan area in southeastern Iran. XRF tests were performed on the volcanic ash, according to ASTM C618-19a (2019), to determine its chemical compounds and the results are shown in Table 3.

3. Soil stabilization and characterization tests

3.1. Equilibrium time

One of the first challenges was to determine the optimum time for carbonation. To this, three types of samples with three different binder contents of 10 wt%, 15 wt%, and 20 wt% (related to the dry soil), and the same relative density of 80% were prepared and cured in oven at 50 °C for 7 d. Then the samples were put in the carbonation cell at the CO_2 gas pressure of 100 kPa. The differential mass of each sample was recorded every 15 min. As the differential mass of the samples is related to the carbonation products when the mass of the sample becomes constant, the optimum carbonation time can be obtained. The efficient time depicted in Fig. 3 for carbonation is 1 h and after that, the mass of the samples does not change significantly.

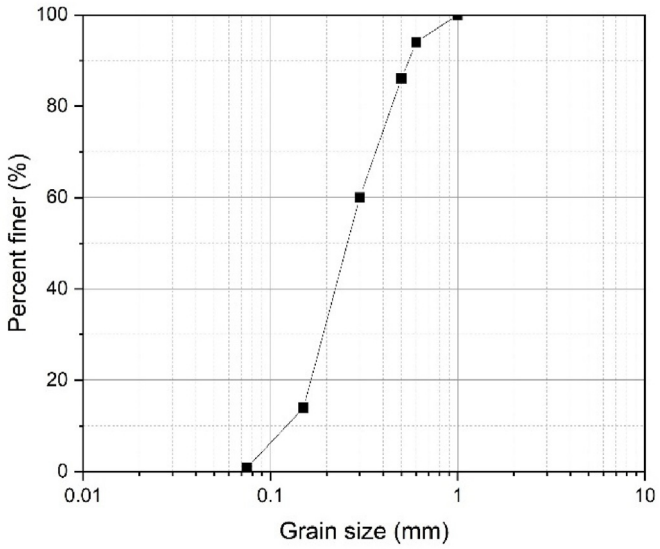

Fig. 1. Grain size distribution curve of Firouzkouh sand.

Table 1
Physical properties of Firouzkouh sand.

Parameter	Value
C_c	1.02
C_u	0.35
D_{60} (mm)	0.38
D_{50} (mm)	0.47
D_{30} (mm)	0.31
D_{10} (mm)	0.2
G_s	2.65
g_{min} (g/cm^3)	1.397
g_{max} (g/cm^3)	1.635

Table 2
Chemical properties of Firouzkouh sand.

Oxide composition	Percentage (%)
SiO_2	94.33
Fe_2O_3	0.9
Al_2O_3	2.03
CaO	1.05
Na_2O	0.49
K_2O	0.21

Table 3
Chemical properties of the volcanic ash.

Oxide composition	Percentage (%)
SiO_2	57.64
Al_2O_3	15.01
CaO	9.51
Na_2O	5.86
Fe_2O_3	4.51
SO3	2.59
MgO	1.97
K_2O	1.8
TiO_2	0.59
P_2O_5	0.23
MnO	0.105

Table 4
The list of the variations in the samples.

Volcanic ash percentage (%)	Relative density (%)	Curing time (day)	Curing condition	CO_2 pressure (atm.)
10	30	3	OC[a]	0[b]
15		7		1
20	80	14	AC[c]	2
25				3

Note: [a] OC condition, [b] Atmospheric condition, [c] AC condition, and 1 atm. = 101.325 kPa.

3.2. Specimen preparation and mechanical characterization

For preparation of the samples for unconfined compressive strength tests, moulds with an internal diameter of 38 mm and a

Please cite this article as: Razeghi HR et al., Effect of CO_2 exposure on the mechanical strength of geopolymer-stabilized sandy soils, Journal of Rock Mechanics and Geotechnical Engineering, https://doi.org/10.1016/j.jrmge.2023.04.017

Fig. 2. Calcimeter instrument used to determine carbonate content.

height/diameter ratio of 2 were utilized. The required soil mass was assumed based on relative density calculation, and relative humidity was assumed 13.5% of soil mass for all the samples. The soil was mixed with volcanic ash for 10 min to obtain a homogeneous blend. In the next step, water, sodium hydroxide, and sodium silicate were mixed according to the geopolymer calculations, and then were added to the mixture of soil and volcanic ash. The whole mixture was stirred for another 10 min to obtain a homogeneous mixture. After blending the materials, the uniform blend was put into the aforementioned mould and compacted in three layers. Three samples were made for each combination of materials. All the samples were cured under two different conditions: AC where the samples were cured at room temperature (20 °C ± 2 °C) and relative humidity 60–80% and OC (OC) in which the samples were placed and cured in an oven at 50 °C. The curing times of specimens were 3 d, 7 d, and 14 d for both curing conditions. After the curing time, the samples were divided into two groups; the first group was placed in the atmospheric condition and the second group was put in the carbonation cell at different CO_2 pressures of 100 kPa, 200 kPa, and 300 kPa for 1 h. Table 4 details all the variations in the samples. After the carbonation time, the unconfined compressive strength tests were conducted on all samples according to the ASTM D1633-17 standard using the strain-controlled method at a pace of 1 mm/min (ASTM D1633-17, 2017). Mechanical tests were performed using a universal testing machine (ELE Digital Tritest 50, ELE Company, Ripley, UK). All the tests were repeated three times, and the average UCS value was reported as the final result.

3.3. Calcimeter test

Calcimeter test was conducted on the carbonated and non-carbonated samples to investigate the amount of carbonation product in the samples according to ISO 10693 (1995). Calcimeter test is performed by means of an instrument, as shown in Fig. 2. The carbonation amount was represented as the equivalent concentration of $CaCO_3$. A specified amount of hydrochloric acid (HCl) first was put in a separate plastic cup and then put in the same reaction vessel with the sample. After the isolation, the hydrochloric acid was poured into the specified amount of sample powder by shaking the reaction vessel. Then some CO_2 gas was released from the sample and the equivalent concentration of $CaCO_3$ was calculated based on the differential pressure produced by the released CO_2 gas. The reaction in simplified form reads as follows (Me means metal):

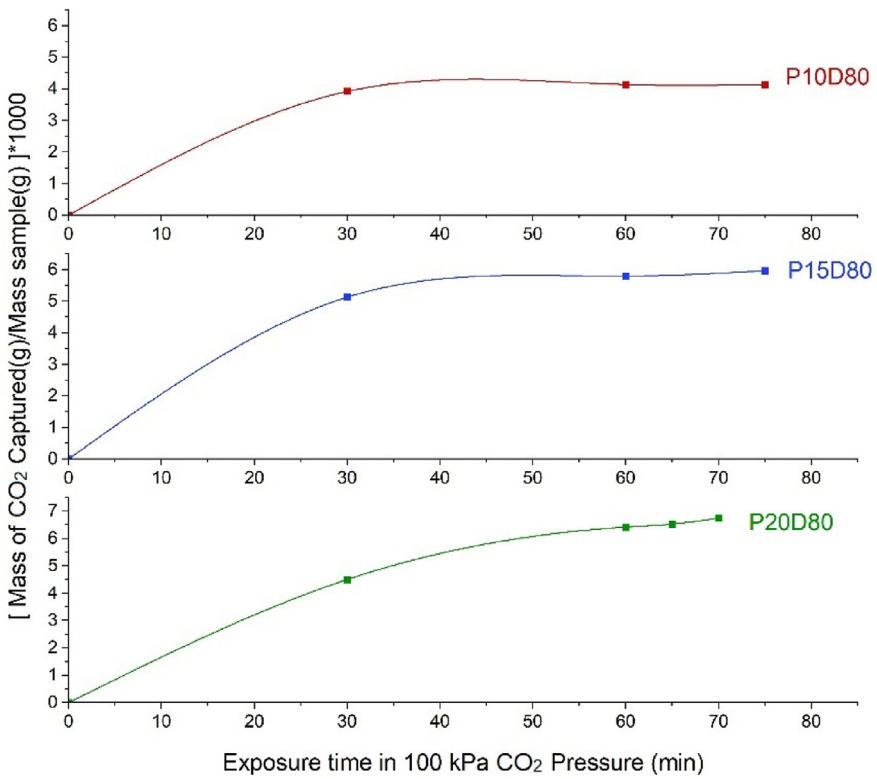

Fig. 3. Equilibrium carbonation time for samples with the same relative density and various binder contents (the number written after P indicates the percentage of binder and the number written after D indicates the relative density of the sample).

Please cite this article as: Razeghi HR et al., Effect of CO_2 exposure on the mechanical strength of geopolymer-stabilized sandy soils, Journal of Rock Mechanics and Geotechnical Engineering, https://doi.org/10.1016/j.jrmge.2023.04.017

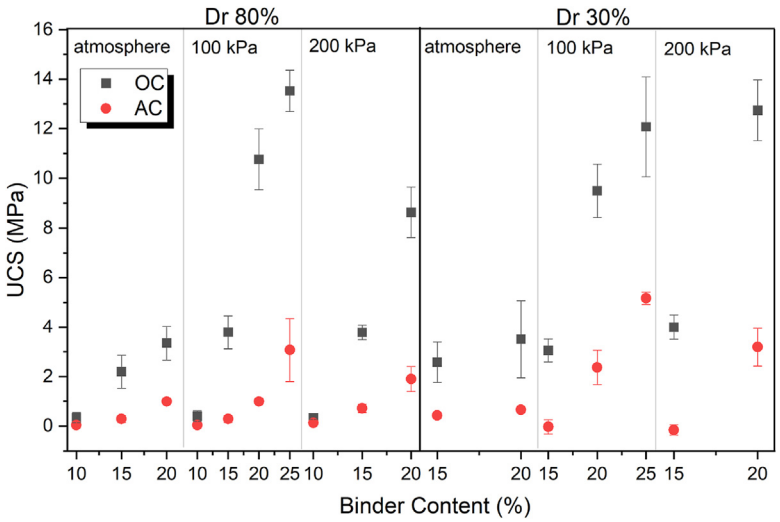

Fig. 4. Unconfined compressive strength of 7-d cured samples at different binder contents, relative densities and curing conditions.

$MeCO_3 + 2H^+ \rightarrow Me^{2+} + H_2CO_3$

$H_2CO_3 \rightarrow H_2O + CO_2$ (gaseous state)

3.4. Microstructural characterization

The carbonated and non-carbonated stabilized soil samples were examined by XRD using X'Pert Pro device of Panalytical Company with anode substance of Cu, a step size of 0.026 and a 2θ range of 2°–80° operated at 40 kV and 40 mA to detect the distinct phases formed by carbonation. Moreover, the powdered samples were squeezed into KBr pellets to be arranged for FTIR examination utilizing an FTIR spectrometer of PerkinElmer Company to distinguish chemical bond structures. SEM-EDS-Mapping via a ZEISS spectroscopy device was used to study the microstructural features of the carbonated and non-carbonated stabilized soil samples.

4. Results

4.1. Compressive strength

Fig. 4 indicates the unconfined compressive strength of 7-d cured samples at different binder contents, relative densities and curing conditions. It can be observed that binder content has a direct relation with UCS in all conditions, but there is large difference in the UCS when the samples were exposed to the CO_2 pressure, especially in 100 kPa. In other words, when the binder content increases, the UCS of the samples increases due to more geopolymeric gel in the atmosphere condition. However, under the influence of CO_2 pressure, the UCS of the samples increases due to both a higher geopolymeric gel content and the presence of additional carbonation products. Additionally, when the samples with low relatively density (30%) are placed in the carbonation cell, they reach the same strength or higher as the samples with a high relative density (80%) in atmospheric condition.

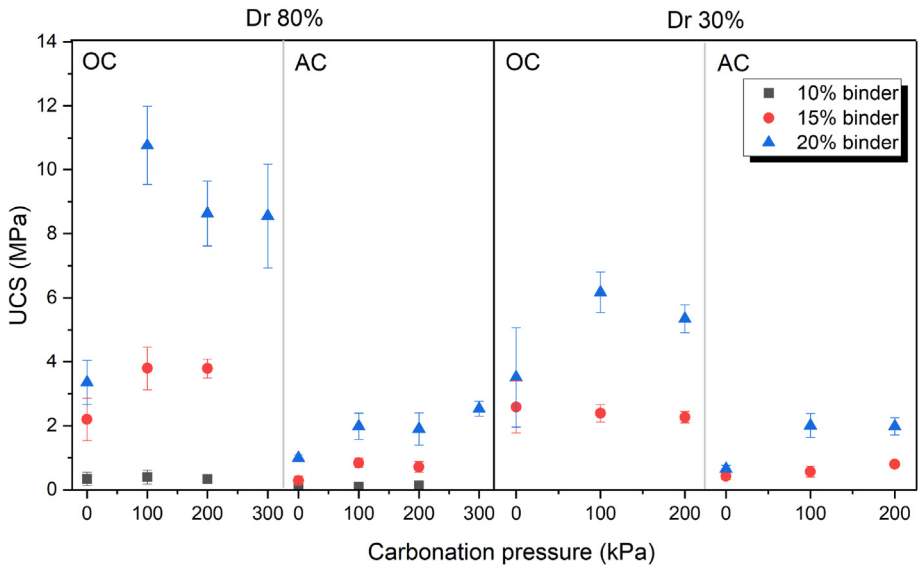

Fig. 5. Unconfined compressive strength of 7-d cured samples at different binder contents, relative densities (Dr) and curing conditions. Dr represents the relative density.

Please cite this article as: Razeghi HR et al., Effect of CO_2 exposure on the mechanical strength of geopolymer-stabilized sandy soils, Journal of Rock Mechanics and Geotechnical Engineering, https://doi.org/10.1016/j.jrmge.2023.04.017

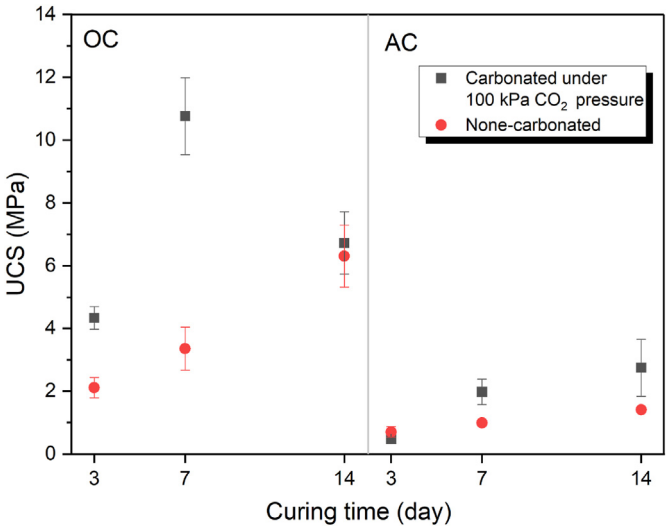

Fig. 6. The effect of curing time on unconfined compressive strength of samples with relative density of 80% and binder content of 20 wt% at different curing conditions.

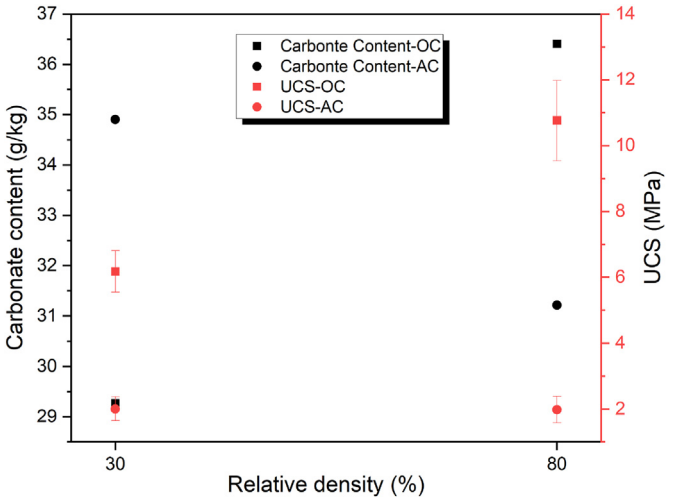

Fig. 8. The effect of relative density on carbonate content and UCS of samples cured for 7 d with binder content of 20 wt% under 100 kPa CO_2 pressure at different curing conditions.

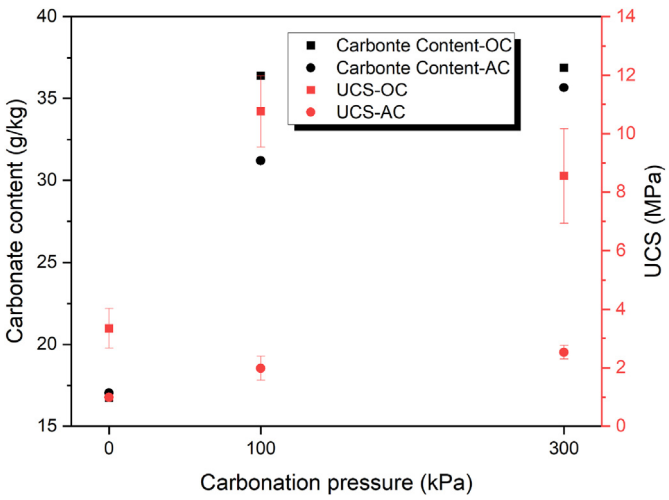

Fig. 7. The effect of CO_2 pressure on carbonate content and UCS of samples cured for 7 d with relative density of 80% and binder content of 20 wt% at different curing conditions.

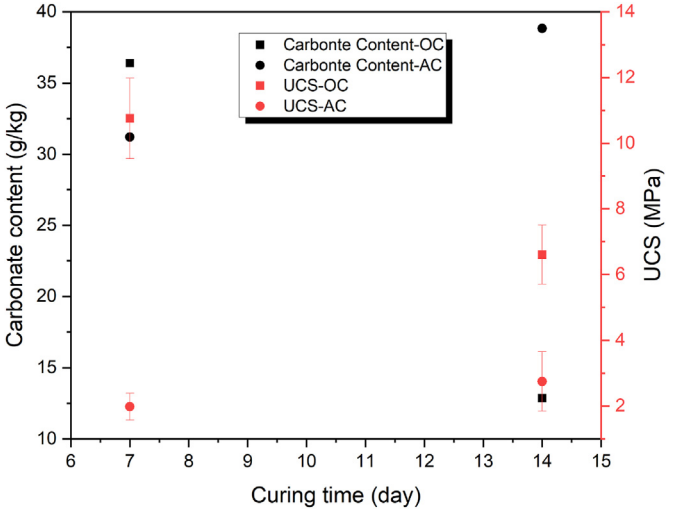

Fig. 9. The effect of curing time on carbonate content and UCS of samples with relative density of 80% and binder content of 20 wt% under 100 kPa CO_2 pressure at different curing conditions.

Fig. 5 shows that the samples stabilized with volcanic ash and cured in oven had higher UCS value because of better performance of natural pozzolan-based geopolymer at high temperatures due to its mineral composition. As can be seen in Fig. 5, there is a considerable difference between the atmosphere condition and the 100 kPa CO_2 pressure condition. However, when the CO_2 pressure increases to 200 kPa and 300 kPa, there is no significant increase in the UCS (1.98 MPa, 1.9 MPa, 2.23 MPa at 100 kPa, 200 kPa, 300 kPa of CO_2 pressure, respectively). In other words, 100 kPa CO_2 pressure is the optimum pressure among the other pressures for gaining strength and 100 kPa of CO_2 pressure is enough for processing all carbonation reactions.

Fig. 6 presents the effect of curing time on mechanical strength of samples with relative density of 80% and binder content of 20 wt %. It is observed that the geopolymerization rate is higher in the first 7 d than other times. In other words, there is a considerable difference in the UCS between 3 d and 7 d but there is a slight difference between 7 d and 14 d in both curing conditions. The other point is that under the atmospheric condition, the UCS increased with curing time in both OC and AC. However, in the OC condition when the samples are exposed to the CO_2 pressure, the increased UCS in the 14-d samples is lower than the 7-d samples. In other words, when the 7-d samples were exposed to the CO_2 pressure, more carbonation product was formed than the 14-d samples. This can be attributed to the lack of water required for the carbonation process in the 14-d samples. However, in the AC condition for the carbonated samples, the expected trend occurred and the UCS increased with increasing the curing time.

4.2. Calcimeter test

Fig. 7 reflects the effect of CO_2 pressure on carbonate content and UCS of the samples cured for 7 d with relative density of 80% and binder content of 20 wt%. Although there is a notable difference among the samples cured under atmospheric condition and those under 100 kPa CO_2 pressure, there is no significant difference between the samples under 100 kPa CO_2 pressure and

Please cite this article as: Razeghi HR et al., Effect of CO_2 exposure on the mechanical strength of geopolymer-stabilized sandy soils, Journal of Rock Mechanics and Geotechnical Engineering, https://doi.org/10.1016/j.jrmge.2023.04.017

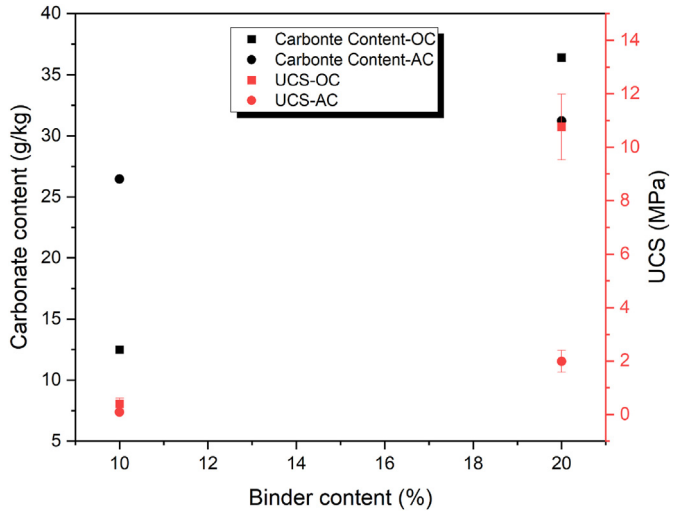

Fig. 10. The effect of binder content on carbonate content and UCS of samples cured for 7 d with relative density of 80% under 100 kPa CO_2 pressure at different curing conditions.

the samples under 300 kPa CO_2 pressure (17.03 g/kg at atmospheric pressure and 31.21 g/kg and 35.67 g/kg at 100 kPa and 300 kPa CO_2 pressure, respectively). Also, the carbonation content results in Fig. 7 confirm this because the carbonate contents of the samples under 100 kPa CO_2 pressure and those under 300 kPa CO_2 pressure are nearly the same but are more than the carbonate content of the atmospheric samples. Moreover, like UCS, the carbonate content has a significant increase in the OC condition because the high temperatures at an early age help to accelerate the geopolymeric reactions and the formation of carbonation product. However, in AC this increase is lower than in OC.

Fig. 8 indicates the effect of relative density on carbonate content and UCS of 7-d cured samples with binder content of 20 wt% under 100 kPa CO_2 pressure. It is demonstrated that in the OC condition, the samples with a low relative density (like 30%) have lower carbonate content than the samples with a high relative density (like 80%) due to the presence of more geopolymeric gel in the latter groups. Also, the UCS results follow the carbonate content results, and the samples with higher relative density have higher UCS value due to the high geopolymerization rate at high temperatures and high density of the samples. However, in the AC condition, the low relative density samples have higher carbonate content than the high relative density samples. The UCS results follow this trend, and the samples with lower relative density have higher UCS value than those with higher relative density. This can be attributed to the presence of more pores in the lower relative density samples and enough water for the carbonation process, which leads to more carbonate content and higher UCS value.

Fig. 9 illustrates the impact of curing time on carbonate content and UCS of samples with relative density of 80% and binder content of 20 wt% under 100 kPa CO_2 pressure. In the OC condition, the water required for the carbonation process is gradually decreased after 7 d of curing time in the oven. This leads to the formation of lower carbonate content in the samples cured for 14 d compared with those cured for 7 d. This in turn results in lower UCS value in the samples cured for 14 d. However, in the AC condition, the geopolymeric and carbonate products continue to form even after 7 d but at lower rate than the first 7 d. As a result, the samples cured for 14 d in AC condition have higher carbonate content and higher UCS value than the samples cured for 7 d.

The effect of binder content on the carbonate content and UCS of samples can be observed in Fig. 10. As expected, the binder content

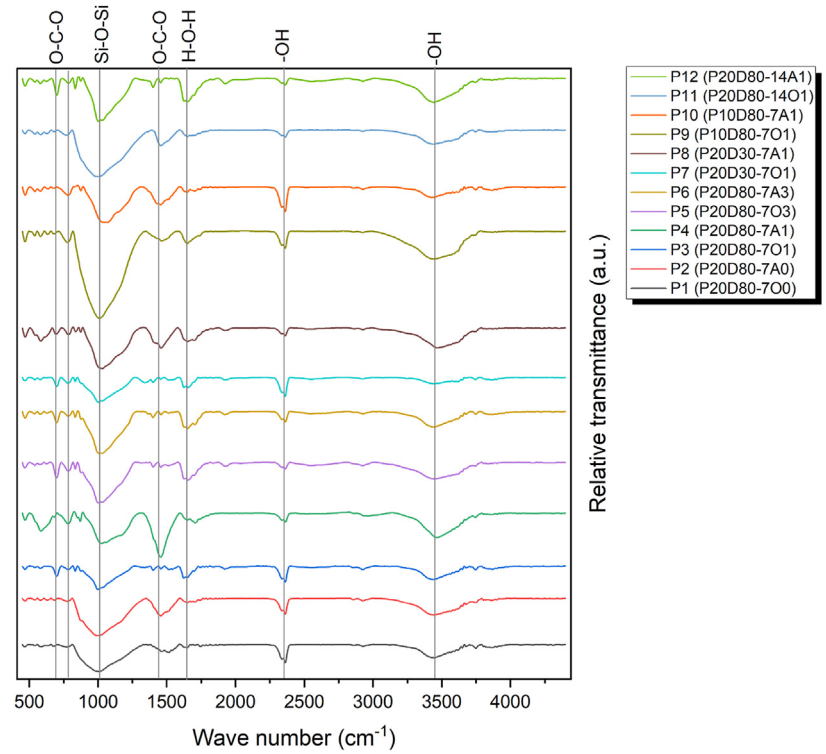

Fig. 11. FTIR spectra of the selected samples (the first number written after the dash indicates curing time and last number shows the CO_2 pressure; and the letter A and O indicates AC and OC conditions, respectively).

Please cite this article as: Razeghi HR et al., Effect of CO_2 exposure on the mechanical strength of geopolymer-stabilized sandy soils, Journal of Rock Mechanics and Geotechnical Engineering, https://doi.org/10.1016/j.jrmge.2023.04.017

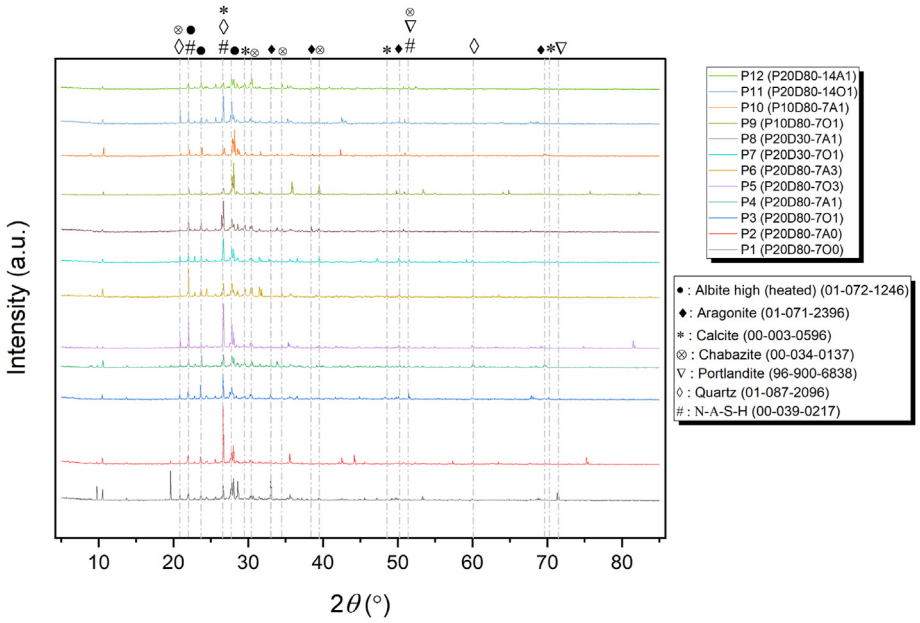

Fig. 12. XRD pattern of selected samples.

has a close relationship with carbonate content and UCS. In other words, at a constant CO_2 pressure, when the binder content increases, more geopolymeric gel and more carbonate content are formed and as a result, the UCS increases. Another point is that in the first 7 d of curing, the effect of curing condition on the rates of geopolymer formation and carbonate formation is considerably high in OC condition due to better performance of volcanic ash in contrast to AC condition.

4.3. FTIR analysis

The FTIR spectra of the selected samples is displayed in Fig. 11. As can be seen, the broad spectrum of 3200–3300 cm^{-1} and the peak at the wavelength of 1600 cm^{-1} belong to the stretching vibration (-OH) and the bending vibration (H-O-H), which are presented in the water molecule (Tchakoute Kouamo et al., 2012). This water may be related to the water on the surface of the sample or the water in the pores of the sample. Also, it can be seen that in the specimens cured in OC conditions (indicated by letter O in the name of the sample in Fig. 11), the peak intensity is lower than that cured in AC conditions (indicated by letter A in the name of the sample in the Fig. 11). This reduction in the peak can be due to the reduction of the vibration related to the bond in the water molecules or due to the reduction of the water molecules in the oven-cured samples (Tchakoute Kouamo et al., 2012; Tchakoute Kouamo et al., 2013a).

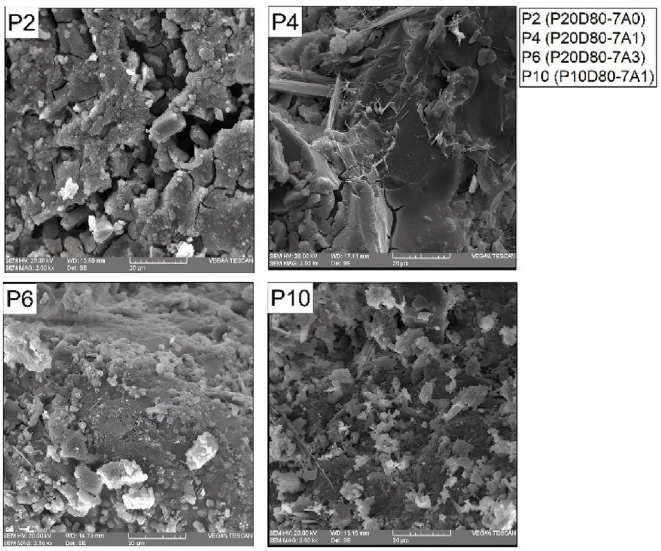

Fig. 13. SEM micrographs of selected samples cured in AC conditions.

In the same way, the peak observed at the wavelength of about 2300 cm^{-1} can be related to −OH bond and the stretching vibration between H and O in the water molecules. The peak at the wavelength of about 2300 cm^{-1} is attributed only to the water absorbed by the geopolymer, but not to the water molecules on the surface; that is why the intensity of this peak is almost the same in all samples (Tchakoute Kouamo et al., 2013a).

There is another peak at a wavelength of about 1000 cm^{-1} related to the formation and activation of the geopolymer gel, especially the O-Si-O bond, which may be considered as a proof of the formation and activation of the geopolymer gel in all selected specimens (Tchakoute Kouamo et al., 2012; Tchakoute Kouamo et al., 2013a; Santos et al., 2021). It can also be observed that the intensity of this peak in the P11 sample that was cured for 14 d is higher than that cured in 7 d because the structure and network of the geopolymer is more complete in 14 d compared to that in 7 d.

The peak related to the wavelength of about 1400 cm^{-1} is attributed to the O-C-O bond, which is related to sodium bicarbonate products (Skocek et al., 2020). The reason for its formation is the absorption of CO_2 gas in the atmosphere by the sample (Santos et al., 2021). The peak at the wavelength of about 700 cm^{-1} is also related to O-C-O bond and the difference with the peak at 1400 cm^{-1} is in the type of vibration of their bonds. In other words, the bond corresponding to the 700 cm^{-1} peak is a kind of in-plane vibration, and the vibration in the 1400 cm^{-1} peak is a kind of out-of-plane vibration. It should also be noted that the intensity of 1400 cm^{-1} and 700 cm^{-1} peaks is reduced in samples P1 and P2. In other words, these samples have a smaller amount of carbonation products. Also, the intensity of the peaks at the pressure of 100 kPa

Please cite this article as: Razeghi HR et al., Effect of CO_2 exposure on the mechanical strength of geopolymer-stabilized sandy soils, Journal of Rock Mechanics and Geotechnical Engineering, https://doi.org/10.1016/j.jrmge.2023.04.017

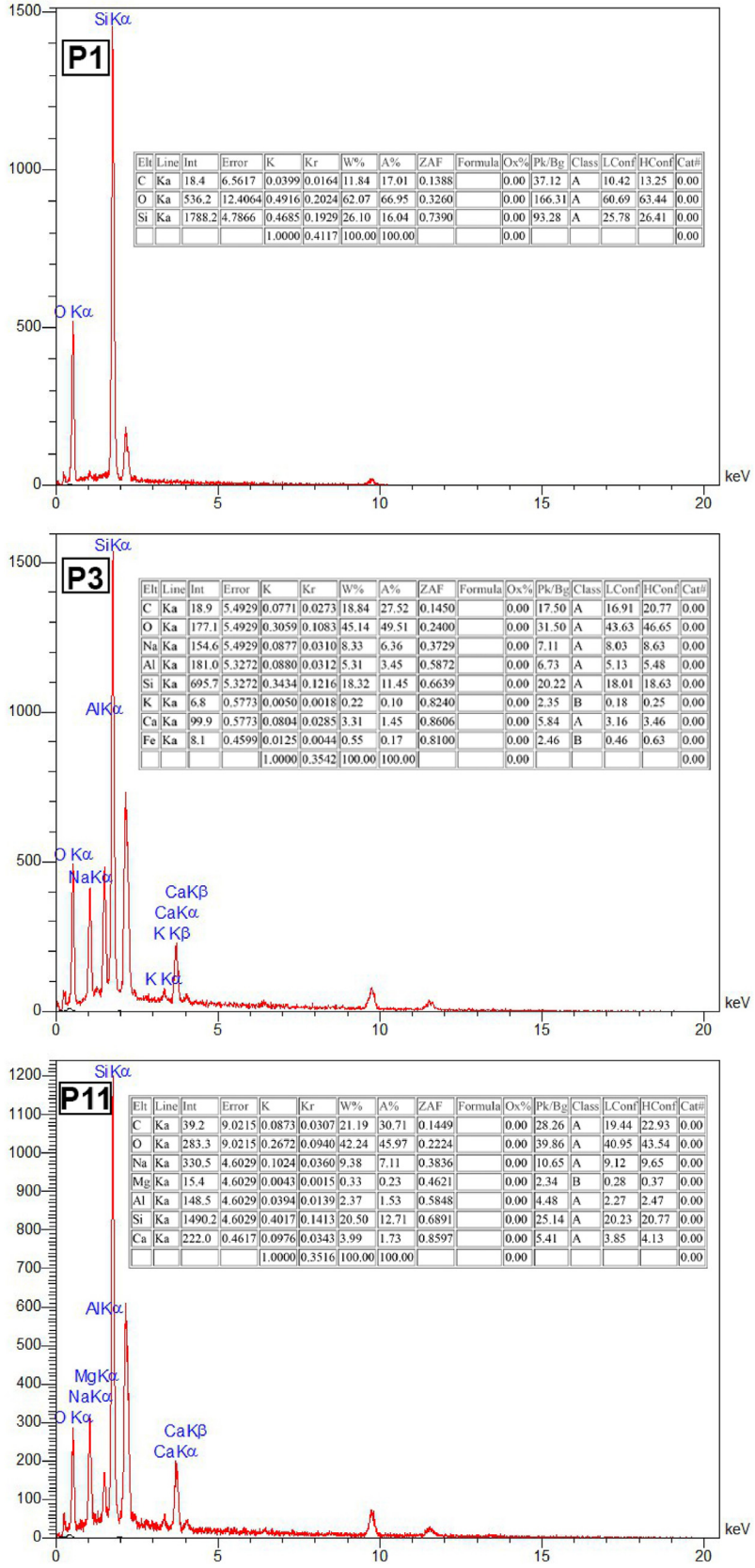

Elt	Line	Int	Error	K	Kr	W%	A%	ZAF	Formula	Ox%	Pk/Bg	Class	LConf	HConf	Cat#
C	Ka	18.4	6.5617	0.0399	0.0164	11.84	17.01	0.1388		0.00	37.12	A	10.42	13.25	0.00
O	Ka	536.2	12.4064	0.4916	0.2024	62.07	66.95	0.3260		0.00	166.31	A	60.69	63.44	0.00
Si	Ka	1788.2	4.7866	0.4685	0.1929	26.10	16.04	0.7390		0.00	93.28	A	25.78	26.41	0.00
				1.0000	0.4117	100.00	100.00			0.00					0.00

Elt	Line	Int	Error	K	Kr	W%	A%	ZAF	Formula	Ox%	Pk/Bg	Class	LConf	HConf	Cat#
C	Ka	18.9	5.4929	0.0771	0.0273	18.84	27.52	0.1450		0.00	17.50	A	16.91	20.77	0.00
O	Ka	177.1	5.4929	0.3059	0.1083	45.14	49.51	0.2400		0.00	31.50	A	43.63	46.65	0.00
Na	Ka	154.6	5.4929	0.0877	0.0310	8.33	6.36	0.3729		0.00	7.11	A	8.03	8.63	0.00
Al	Ka	181.0	5.3272	0.0880	0.0312	5.31	3.45	0.5872		0.00	6.73	A	5.13	5.48	0.00
Si	Ka	695.7	5.3272	0.3434	0.1216	18.32	11.45	0.6639		0.00	20.22	A	18.01	18.63	0.00
K	Ka	6.8	0.5773	0.0050	0.0018	0.22	0.10	0.8240		0.00	2.35	B	0.18	0.25	0.00
Ca	Ka	99.9	0.5773	0.0804	0.0285	3.31	1.45	0.8606		0.00	5.84	A	3.16	3.46	0.00
Fe	Ka	8.1	0.4599	0.0125	0.0044	0.55	0.17	0.8100		0.00	2.46	B	0.46	0.63	0.00
				1.0000	0.3542	100.00	100.00			0.00					0.00

Elt	Line	Int	Error	K	Kr	W%	A%	ZAF	Formula	Ox%	Pk/Bg	Class	LConf	HConf	Cat#
C	Ka	39.2	9.0215	0.0873	0.0307	21.19	30.71	0.1449		0.00	28.26	A	19.44	22.93	0.00
O	Ka	283.3	9.0215	0.2672	0.0940	42.24	45.97	0.2224		0.00	39.86	A	40.95	43.54	0.00
Na	Ka	330.5	4.6029	0.1024	0.0360	9.38	7.11	0.3836		0.00	10.65	A	9.12	9.65	0.00
Mg	Ka	15.4	4.6029	0.0043	0.0015	0.33	0.23	0.4621		0.00	2.34	B	0.28	0.37	0.00
Al	Ka	148.5	4.6029	0.0394	0.0139	2.37	1.53	0.5848		0.00	4.48	A	2.27	2.47	0.00
Si	Ka	1490.2	4.6029	0.4017	0.1413	20.50	12.71	0.6891		0.00	25.14	A	20.23	20.77	0.00
Ca	Ka	222.0	0.4617	0.0976	0.0343	3.99	1.73	0.8597		0.00	5.41	A	3.85	4.13	0.00
				1.0000	0.3516	100.00	100.00			0.00					0.00

Fig. 14. EDS analysis of selected samples cured in OC conditions.

Please cite this article as: Razeghi HR et al., Effect of CO_2 exposure on the mechanical strength of geopolymer-stabilized sandy soils, Journal of Rock Mechanics and Geotechnical Engineering, https://doi.org/10.1016/j.jrmge.2023.04.017

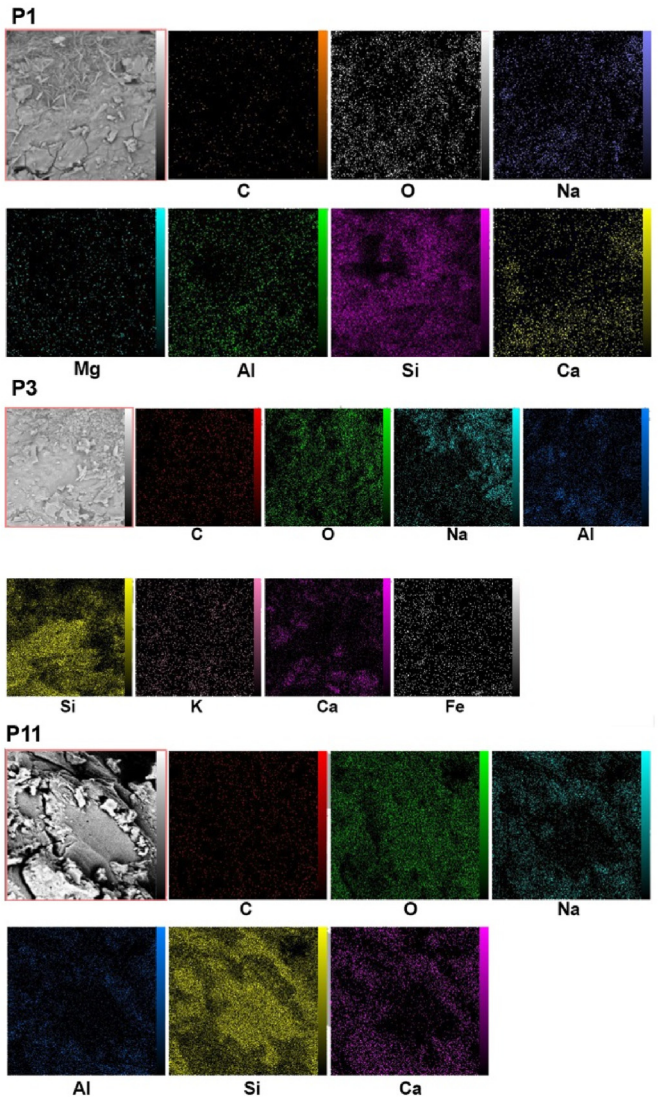

Fig. 15. Elemental mapping analysis of selected samples cured in OC conditions.

of CO_2 confirms the mechanical and calcimeter parts that this pressure is the optimal pressure for absorption (Tchakoute Kouamo et al., 2012; Skocek et al., 2020; Santos et al., 2021).

4.4. XRD analysis

The XRD pattern of carbonated and non-carbonated samples in both oven and AC conditions is presented in Fig. 12. Many crystalline peaks can be seen, indicating the presence of N-A-S-H, Albite high (heated), quartz and chabazite can be formed in all samples due to the syntheses of geopolymer materials from natural aluminosilicate (Sindhunata et al., 2006; Chen et al., 2018; Zhang et al., 2019). Calcite is one of the main products after carbonation, and it is observed in P3 (P20D80-7O1) and P4 (P20D80-7A1) due to the carbonation time (Cai et al., 2016; Shariatmadari et al., 2021a; Zhong et al., 2021). Another main product of the carbonation process with different crystalline structure is aragonite tracked in P3 and P4 samples. Although it is expected that vaterite would be the first crystalline peak of $CaCO_3$ during the carbonation, vaterite has been converted to calcite and aragonite phases due to its instability (Mo and Panesar, 2012; Zhang et al., 2019). Also, hydrated minerals such as portlandite are observed which is prone to reacting during carbonation. However, the portlandite peaks are weak due to slow hydration rate of volcanic ash. Portlandite peaks gradually disappear because of the conversion of $Ca(OH)_2$ into calcite and aragonite after carbonation in carbonated samples (Huijgen et al., 2006; Özbay et al., 2016; Wang et al., 2019; Zhong et al., 2021). Generally, it can be seen that the intensity of peaks has been weakened in P9 (P10D80-7O1) and P10 (P10D80-7A1) with respect to P3 (P20D80-7O1) and P4 (P20D80-7A1), due to less binder content of volcanic ash which leads to less geopolymeric gel and carbonate content (Wang et al., 2019). It is also observed that crystalline structures of P5 (P20D80-7O3) and P6 (P20D80-7A3) are not much different from P3 (P20D80-7O1) and P4 (P20D80-7A1), although they are placed in different CO_2 pressures. Therefore, it can be concluded that the CO_2 pressure of 100–300 kPa has no significant difference in the results and the pressure of 100 kPa can be considered as the optimal pressure for gaining strength and precipitating carbonation products (Fasihnikoutalab et al., 2016, 2017a).

4.5. SEM-EDS characterization

The SEM micrographs of the samples cured in AC conditions is shown in Fig. 13. As observed in the XRD results, geopolymer gels (including quartz and albite phases) are formed in P2 specimen (see Fig. 13a). In P4 specimen, a carbonated sample under 100 kPa CO_2 pressure, the phases resulting from the CO_2 exposure such as calcite and aragonite can be seen with rhombohedral, cubical, and needle-like structures, respectively (Wong et al., 2020; Mohammed et al., 2021). Aragonite is usually formed in relative high temperatures

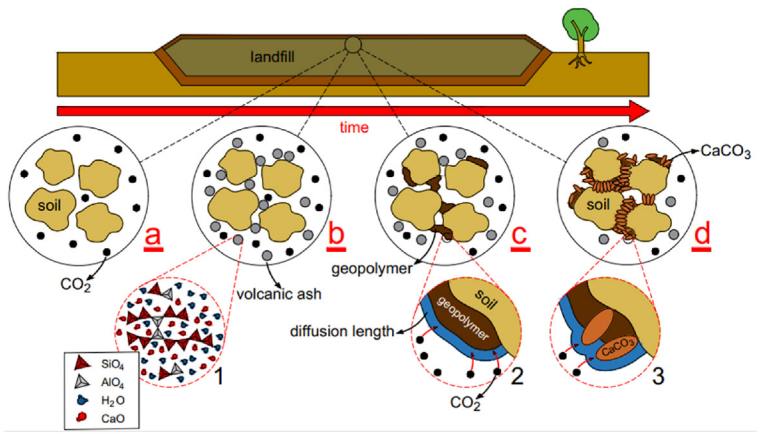

Fig. 16. Schematic diagram of carbonation using volcanic ash in hypothetical project.

Please cite this article as: Razeghi HR et al., Effect of CO_2 exposure on the mechanical strength of geopolymer-stabilized sandy soils, Journal of Rock Mechanics and Geotechnical Engineering, https://doi.org/10.1016/j.jrmge.2023.04.017

in comparison with calcite (Mohammed et al., 2021). The microstructure and morphology of P6 and P4 samples are similar, although they experience different CO_2 pressures (Fig. 13b-c). Blocky calcite structure is the dominant structure in both samples (Song et al., 2017; Hu et al., 2018). The less amount of binder content resulted in less compact microstructure of P10 specimen with 10 wt% binder content in comparison with P4 specimen with 20 wt % binder content (Fig. 13d). In other words, the phases resulting from carbonation are not fully developed in P10 compared to P4 (Wang et al., 2019; Liu and Meng, 2021).

EDS and elemental mapping analyses of three samples P1, P3 and P11, cured in OC conditions are shown in Figs. 14 and 15, respectively. It can be observed that in sample P1, which is a non-carbonated sample, only geopolymeric gels are formed and silicon and oxygen and carbon elements in this sample have a high content. However, for sample P3, it is similar to sample P1 in its constituent materials, but carbonated under 100 kPa of CO_2 gas pressure. It can be seen that the percentage of elements forming carbonate compounds (such as calcium) has increased and the N-A-S-H gel has been formed in a larger amount in the sample P3 than the sample P1 because of broad distribution of alkaline metals like Na according to Fig. 15 (Minelli et al., 2016; Ghadir and Razeghi, 2022). Although sample P11 is similar to sample P3 in all cases except for the curing time (sample P3 cured for 7 d and sample P11 for 14 d), it should be noted that in sample P11, the water needed for carbonation and forming carbonated products has disappeared. For this, the percentage of carbonated compound elements has decreased compared to sample P3 (Vandeperre and Al-Tabbaa, 2007; Minelli et al., 2016; Özbay et al., 2016).

5. Discussion

In order to elaborate on the CO_2 exposure effect, Fig. 16 proposes a hypothetical project as a landfill where a considerable amount of CO_2 is released. Therefore, the carbonation process can be implemented to stabilize the cover layer of the landfill. Fig. 16 illustrates the carbonation in four general stages. Fig. 16a shows the soil particles exposed to CO_2 gas. In the second stage, the volcanic ash and an alkali activator (including water) are added to the soil, as shown in Fig. 16b. The alkali activator like water activates the geopolymer based on volcanic ash by breaking the bond Si-O and Al-O, resulting in forming N-A-S-H gel as shown in Fig. 16c (Ghadir et al., 2021; Miraki et al., 2022). Note that the CO_2 cannot react with free ions like Ca^{2+} directly, so the CO_2 dissolved in a thin layer of moisture called diffusion length surrounding the volcanic ash particle which leads to the formation of H_2CO_3 as shown in Fig. 16c (2) (Kim and Kwon, 2019). In the fourth and final stage, the carbonation products like $CaCO_3$ are formed and bind the soil particles in combination with N-A-S-H gel in geopolymer base volcanic ash.

6. Conclusions

This study evaluated the effect of CO_2 exposure on the mechanical features of sandy soil stabilized with volcanic ash-based geopolymer. It was demonstrated that CO_2 exposure has a promising positive effect on the mechanical properties of sandy soils stabilized with volcanic ash based geopolymer. The following conclusions can be obtained from the results presented in this study:

(1) The amount of carbonate and bicarbonate products directly depend on the binder content of the samples and it increases with increasing volcanic ash content up to about 30 wt%.

(2) From the quantitative perspective of carbonation products, the findings suggest that there is no significant difference between the pressure of 100–300 kPa of CO_2. As a result, it can be inferred that the saturation point of CO_2 is reached at a certain pressure level, indicating no further increase in soil strength. In essence, the sample attains a state of CO_2 saturation, characterized by no further capacity for additional strength.

(3) Volcanic ash based geopolymer has an optimum performance and higher mechanical strength in OC than that in AC condition. In other words, the carbonation process is more efficient and produces more carbonate and bicarbonate compounds in OC conditions. However, in the OC condition, after 7 d curing, the required water for carbonation gradually decreases and the carbonation process is not as efficient as in the first 7-d curing age.

(4) In a low relative density, the pores of the sample are larger and allow more CO_2 molecules to penetrate the sample in order to form carbonate and bicarbonate compounds.

(5) No considerable difference is observed among various CO_2 pressures in the strength development of carbonated samples. As a result, 100 kPa of CO_2 pressure can be considered the optimum pressure for carbonation among the others because of lower cost and lower energy requirement.

Declaration of competing interest

The authors declare that they have no known competing financial interests or personal relationships that could have appeared to influence the work reported in this paper.

Acknowledgment

The authors would like to appreciate the efforts of Eng. Salar Khoramdel and Professor Nader Shariatmadari (RIP). This study was supported by MatSoil Company (Grant No. 04G/2022). This research was funded by the European Union's Horizon 2020 research and innovation program under the Marie Sklodowska-Curie (Grant No. 778120).

References

ASTM C618-19a, 2019. Standard Specification for Coal Fly Ash and Raw or Calcined Natural Pozzolan for Use in Concrete. ASTM International, West Conshohocken, PA, USA.

ASTM D422-63, 2002. Standard Test Method for Particle-Analysis of Soils. ASTM International, West Conshohocken, PA, USA.

ASTM D1633-17, 2017. Standard Test Methods for Compressive Strength of Molded Soil-Cement Cylinders. ASTM International, West Conshohocken, PA, USA.

ASTM D698-21, 2021. Standard Test Methods for Laboratory Compaction Characteristics of Soil Using Standard Effort (12,400 Ft-Lbf/ft3 (600 kN-M/m^3. ASTM International, West Conshohocken, PA, USA.

Cai, G., Noguchi, T., Degée, H., Zhao, J., Kitagaki, R., 2016. Volcano-related materials in concretes: a comprehensive review. Environ. Sci. Pollut. Res. 23 (10), 7220–7243.

Chen, Z., Li, J.S., Zhan, B.J., Sharma, U., Poon, C.S., 2018. Compressive strength and microstructural properties of dry-mixed geopolymer pastes synthesized from GGBS and sewage sludge ash. Construct. Build. Mater. 182, 597–607.

Cheng-Yong, H., Yun-Ming, L., Abdullah, M.M.A.B., Hussin, K., 2017. Thermal resistance variations of fly ash geopolymers: foaming responses. Sci. Rep. 7, 1–11.

Djobo, J.N.Y., Elimbi, A., Tchakouté, H.K., Kumar, S., 2017. Volcanic ash-based geopolymer cements/concretes: the current state of the art and perspectives. Environ. Sci. Pollut. Res. 24, 4433–4446.

Fasihnikoutalab, M.H., Asadi, A., Huat, B.K., Ball, R.J., Pourakbar, S., Singh, P., 2017a. Utilisation of carbonating olivine for sustainable soil stabilization. Environ. Geotech. 4, 184–198.

Fasihnikoutalab, M.H., Asadi, A., Kim Huat, B., Westgate, P., Ball, R.J., Pourakbar, S., 2016. Laboratory-scale model of carbon dioxide deposition for soil stabilisation. J. Rock Mech. Geotech. Eng. 8, 178–186.

Fasihnikoutalab, M.H., Asadi, A., Unluer, C., Huat, B.K., Ball, R.J., Pourakbar, S., 2017b. Utilization of alkali-activated olivine in soil stabilization and the effect of

carbonation on unconfined compressive strength and microstructure. J. Mater. Civ. Eng. 29, 1–11.
Ghadir, P., Ranjbar, N., 2018. Clayey soil stabilization using geopolymer and Portland cement. Construct. Build. Mater. 188, 361–371.
Ghadir, P., Razeghi, H.R., 2022. Effects of sodium chloride on the mechanical strength of alkali activated volcanic ash and slag pastes under room and elevated temperatures. Construct. Build. Mater. 344, 128113.
Ghadir, P., Zamanian, M., Mahbubi-Motlagh, N., Saberian, M., Li, J., Ranjbar, N., 2021. Shear strength and life cycle assessment of volcanic ash-based geopolymer and cement stabilized soil: a comparative study. Transp. Geotech. 31, 100639.
He, M., Luis, S., Rita, S., Ana, G., Euripedes, V., Zhang, N., 2011. Risk assessment of CO2 injection processes and storage in carboniferous formations: a review. J. Rock Mech. Geotech. Eng. 3, 39–56.
Hu, W., Nie, Q., Huang, B., Su, A., Du, Y., Shu, X., et al., 2018. Mechanical property and microstructure characteristics of geopolymer stabilized aggregate base. Construct. Build. Mater. 191, 1120–1127.
Huijgen, W.J.J., Ruijg, G.J., Comans, R.N.J., Witkamp, G.J., 2006. Energy consumption and net CO2 sequestration of aqueous mineral carbonation. Ind. Eng. Chem. Res. 45, 9184–9194.
ISO 10693, 1995. In: Soil Quality—Determination of Carbonate Content—Volumetric Method, vol. 10693. International Organization for Standardization, p. 1995.
Kim, J.H., Kwon, W.T., 2019. Semi-dry carbonation process using fly ash from solid refused fuel power plant. Sustain. Times 11 (3), 908.
Lim, M., Han, G.C., Ahn, J.W., You, K.S., 2010. Environmental remediation and conversion of carbon dioxide (CO2) into useful green products by accelerated carbonation technology. Int. J. Environ. Res. Publ. Health 7, 203–228.
Liu, Z., Meng, W., 2021. Fundamental understanding of carbonation curing and durability of carbonation-cured cement-based composites: a review. J. CO2 Util. 44, 101428.
Lu, H.Y., Lin, C.K., Lin, W., Liou, T.S., Chen, W.F., Chang, P.Y., 2011. A natural analogue for CO2 mineral sequestration in Miocene basalt in the Kuanhsi-Chutung area, Northwestern Taiwan. Int. J. Greenh. Gas Control 5, 1329–1338.
Minelli, M., Medri, V., Papa, E., Miccio, F., Landi, E., Doghieri, F., 2016. Geopolymers as solid adsorbent for CO2 capture. Chem. Eng. Sci. 148, 267–274.
Miraki, H., Shariatmadari, N., Ghadir, P., Jahandari, S., Tao, Z., Siddique, R., 2022. Clayey soil stabilization using alkali-activated volcanic ash and slag. J. Rock Mech. Geotech. Eng. 14 (3), 576–591.
Mo, L., Panesar, D.K., 2012. Effects of accelerated carbonation on the microstructure of Portland cement pastes containing reactive MgO. Cement Concr. Res. 42, 769–777.
Mohammed, M.A., Mohd Yunus, N.Z., Hezmi, M.A., Abang Hasbollah, D.Z., A Rashid, A.S., 2021. Ground improvement and its role in carbon dioxide reduction: a review. Environ. Sci. Pollut. Res. 28, 8968, 888.
Mohebbi, H.R., Javadi, A.A., Azizkandi, A.S., 2022. The effects of soil porosity and mix design of volcanic ash-based geopolymer on the surface strength of highly wind-erodible soils. Minerals 12 (8), 984.
Mola-Abasi, H., Shooshpasha, I., 2016. Influence of zeolite and cement additions on mechanical behavior of sandy soil. J. Rock Mech. Geotech. Eng. 8 (6), 746–752.
Özbay, E., Erdemir, M., Ibrahim, H., 2016. Utilization and efficiency of ground granulated blast furnace slag on concrete properties – a review. Construct. Build. Mater. 105, 423–434.
Papa, E., Medri, V., Paillard, C., Contri, B., Natali Murri, A., Vaccari, A., et al., 2019. Geopolymer-hydrotalcite composites for CO2 capture. J. Clean. Prod. 237, 117738.
Pavithra, P., Srinivasula Reddy, M., Dinakar, P., Hanumantha Rao, B., Satpathy, B.K., Mohanty, A.N., 2016. A mix design procedure for geopolymer concrete with fly ash. J. Clean. Prod. 133, 117–125.
Razeghi, H.R., Ghadir, P., Javadi, A.A., 2022. Mechanical strength of saline sandy soils stabilized with alkali-activated cements. Sustainability 14 (20), 13669.
Ruan, S., Unluer, C., 2016. Comparative life cycle assessment of reactive MgO and Portland cement production. J. Clean. Prod. 137, 258–273.
Samadi, P., Ghodrati, A., Ghadir, P., Javadi, A.A., 2023. Effect of seawater on the mechanical strength of geopolymer/cement stabilized sandy soils. In: Proceedings of the TMIC 2022 Slope Stability Conference (TMIC 2022). Atlantis Press International BV, Dordrecht, pp. 121–129.
Santos, V.H.J.M., dos, Pontin, D., Ponzi, G.G.D., Stepanha, A.S. de G., Martel, R.B., Schütz, M.K., et al., 2021. Application of FourierTransform infrared spectroscopy (FTIR) coupled with multivariate regression for calcium carbonate ($CaCO_3$) quantification in cement. Construct. Build. Mater. 313, 125466.
Shariatmadari, N., Hasanzadehshooiili, H., Ghadir, P., Saeidi, F., Moharami, F., 2021a. Compressive strength of sandy soils stabilized with alkali-activated volcanic ash and slag. J. Mater. Civ. Eng. 33 (8), 04021295.
Shariatmadari, N., Mohebbi, H.R., Ghadir, P., Jahandari, S., Siddique, R., 2021b. Influence of nano-silicaon the mechanical behavior of alkali-activated volcanic ash and slag stabilized sandy soils. Geotech. Geol. Eng. 39 (5), 4167–4183.
Sindhunata, A., van Deventer, J.S.J., Lukey, G.C., Xu, H., 2006. Effect of curing temperature and silicate concentration on fly-ash-based geopolymerization. Ind. Eng. Chem. Res. 45 (10), 3559–3568.
Skocek, J., Zajac, M., Ben Haha, M., 2020. Carbon capture and utilization by mineralization of cement pastes derived from recycled concrete. Sci. Rep. 10, 20511.
Song, M., Jiaping, L., Wei, L., Wang, Y., Liu, J., Shi, L., et al., 2017. Property and microstructure of aluminosilicate inorganic coating for concrete: role of water to solid ratio. Construct. Build. Mater. 148, 846–856.
Tchakoute Kouamo, H., Elimbi, A., Mbey, J.A., Ngally Sabouang, C.J., Njopwouo, D., 2012. The effect of adding alumina-oxide to metakaolin and volcanic ash on geopolymer products: a comparative study. Construct. Build. Mater. 35, 960–969.
Tchakoute Kouamo, H., Elimbi, A., Yanne, E., Djangang, C.N., 2013a. Utilization of volcanic ashes for the production of geopolymers cured at ambient temperature. Cem. Concr. Compos. 37, 108–116.
Tchakoute Kouamo, H., Mbey, J.A., Elimbi, A., Diffo, B.B.K., Njopwouo, D., 2013b. Synthesis of volcanic ash-based geopolymer mortars by fusion method: effects of adding metakaolin to fused volcanic ash. Ceram. Int. 39 (2), 1613–1621.
Vandeperre, L.J., Al-Tabbaa, A., 2007. Accelerated carbonation of reactive MgO cements. Adv. Cement Res. 19 (2), 67–79.
Wang, D., Zhu, J., He, F., 2019. CO2 carbonation-induced improvement in strength and microstructure of reactive MgO-CaO-fly ash-solidified soils. Construct. Build. Mater. 229, 116914.
Washbourne, C.L., Renforth, P., Manning, D.A.C., 2012. Investigating carbonate formation in urban soils as a method for capture and storage of atmospheric carbon. Sci. Total Environ. 431, 166–175.
Wong, J.K.H., Kok, S.T., Wong, S.Y., 2020. Fibers, geopolymers, nano and alkali-activated materials for deep soil mix binders. Civ. Eng. J. 6 (5), 830–847.
Xu, H., van Deventer, J.S.J., 2000. The geopolymerisation of alumino-silicate minerals. Int. J. Miner. Process. 59 (3), 247–266.
Zhang, M., Guo, H., El-Korchi, T., Zhang, G., Tao, M., 2013. Experimental feasibility study of geopolymer as the next-generation soil stabilizer. Construct. Build. Mater. 47, 1468–1478.
Zhang, J., Shi, C., Zhang, Z., 2019. Carbonation induced phase evolution in alkali-activated slag/fly ash cements: the effect of silicate modulus of activators. Construct. Build. Mater. 223, 566–582.
Zhong, X., Li, L., Jiang, Y., Ling, T.C., 2021. Elucidating the dominant and interaction effects of temperature, CO2 pressure and carbonation time in carbonating steel slag blocks. Construct. Build. Mater. 302, 124158.

Hamid Reza Razeghi obtained his BSc degree in Civil Engineering and MSc degree in Geotechnical Engineering from Iran University of Science and Technology (IUST) in Iran and PhD in Geotechnical Engineering from Tohoku University in Japan. He is an associate professor in IUST and has been involved in geotechnical and geo-environmental researches. Also, he has rich experiences in soil reinforcement and physical modelling projects. He is the author or co-author of more than 50 scientific papers.

Please cite this article as: Razeghi HR et al., Effect of CO_2 exposure on the mechanical strength of geopolymer-stabilized sandy soils, Journal of Rock Mechanics and Geotechnical Engineering, https://doi.org/10.1016/j.jrmge.2023.04.017